



Supplement of

Measurement report: Analysis of aerosol optical depth variation at Zhongshan Station in Antarctica

Lijing Chen et al.

Correspondence to: Huizheng Che (chehz@cma.gov.cn) and Minghu Ding (dingminghu@foxmail.com)

The copyright of individual parts of the supplement might differ from the article licence.

Supplementary Information

List of figures:

Figure S1. Number of observation data obtained from CE318-T at Zhongshan Station in (a) 2020, (b) 2021, (c) 2022, and (d) 2023, respectively.

Figure S2. (a)-(h) the frequency histograms of aerosol optical depth at 500 nm ($AOD_{500\text{ nm}}$) and Angstrom exponent at 440-870 nm ($AE_{440-870\text{ nm}}$) in spring, summer, autumn, and winter, respectively. The red dashed lines represent the lognormal fit curves in (a)-(d), and the normal fit curves in (e)-(h), respectively.

Figure S3. Time series of diurnal variations of $AOD_{500\text{ nm}}$ and $AE_{440-870\text{ nm}}$ on (a) high AOD days, and (b) low AOD days, respectively. The solid blue lines represent $AOD_{500\text{ nm}}$ and the solid red lines represent $AE_{440-870\text{ nm}}$.

Figure S4. HYSPLIT backward trajectory of (a) low AOD days and (b) high AOD days.

List of tables:

Table S1. Dates are classified as low AOD days and high AOD days, respectively. Note: The fifth percentile value of the AOD daily mean is 0.02446, and days with an AOD daily mean below this value are classified as low AOD days; The 95th percentile value of the AOD daily mean is 0.14739, and days with an AOD daily mean above this value are classified as high AOD days.

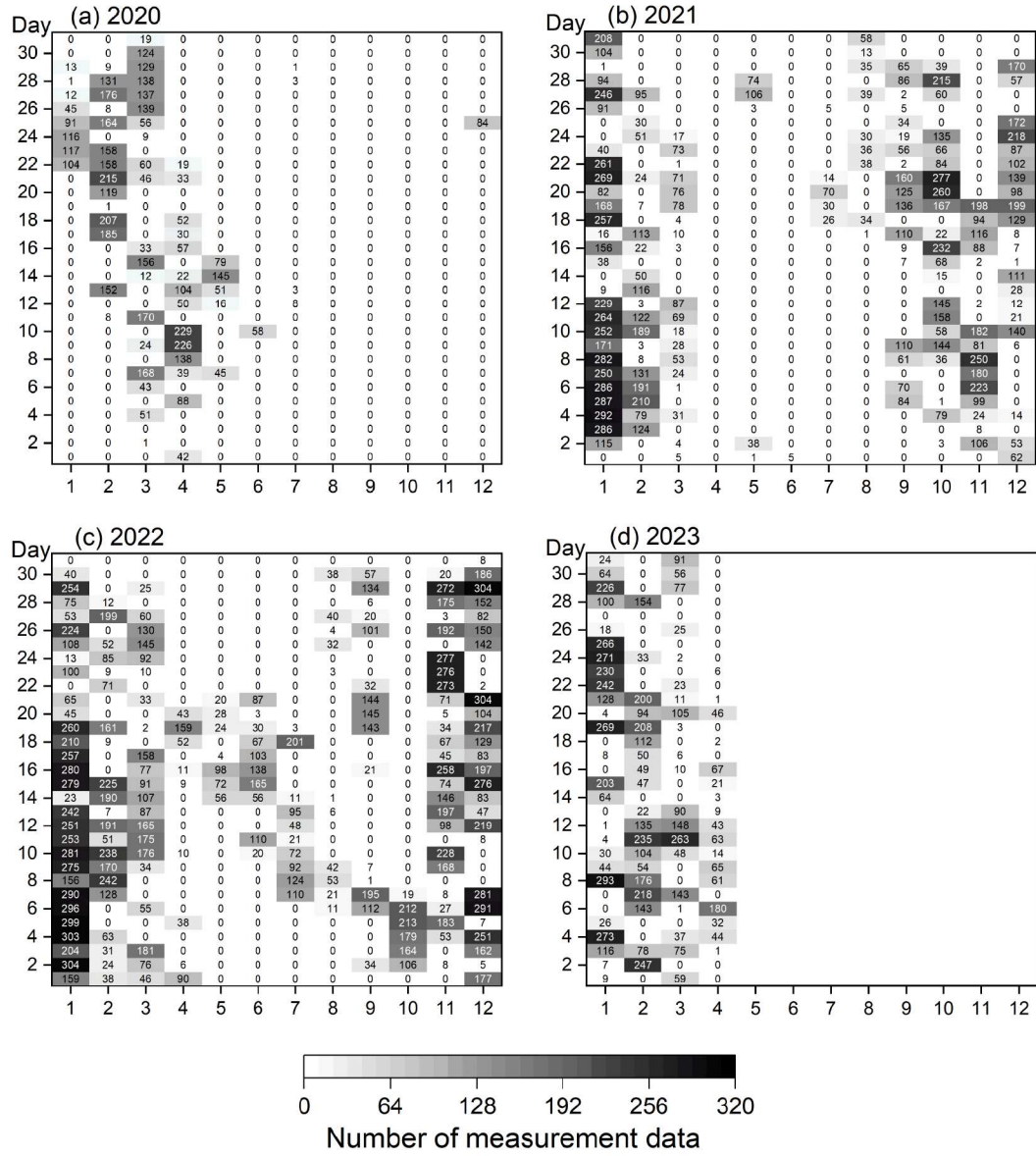


Figure S1. Number of observation data obtained from CE318-T at Zhongshan Station in (a) 2020, (b) 2021, (c) 2022, and (d) 2023, respectively.

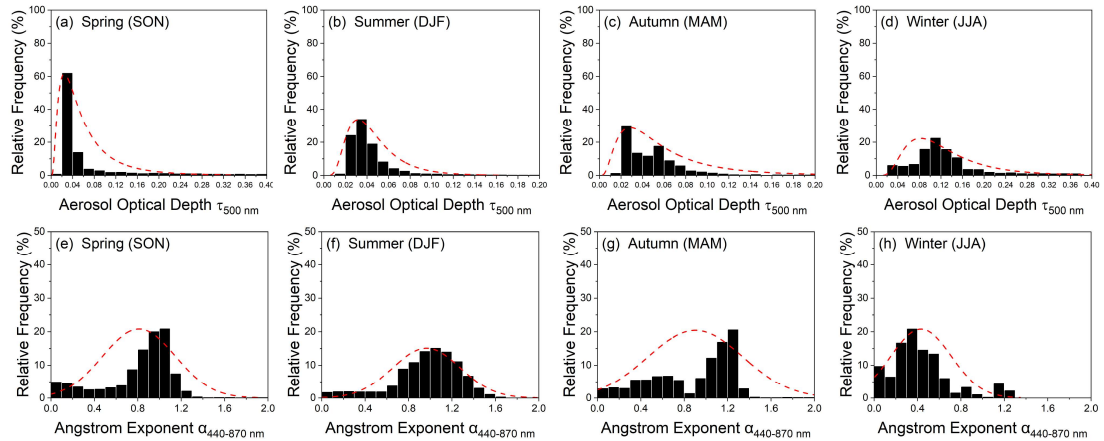


Figure S2. (a)-(h) the frequency histograms of aerosol optical depth at 500 nm ($AOD_{500\text{ nm}}$) and

Angstrom exponent at 440-870 nm ($AE_{440-870 \text{ nm}}$) in spring, summer, autumn, and winter, respectively. The red dashed lines represent the lognormal fit curves in (a)-(d), and the normal fit curves in (e)-(h), respectively.



Figure S3. Time series of diurnal variations of $AOD_{500 \text{ nm}}$ and $AE_{440-870 \text{ nm}}$ on (a) high AOD days, and (b) low AOD days, respectively. The solid blue lines represent $AOD_{500 \text{ nm}}$ and the solid red lines represent $AE_{440-870 \text{ nm}}$.

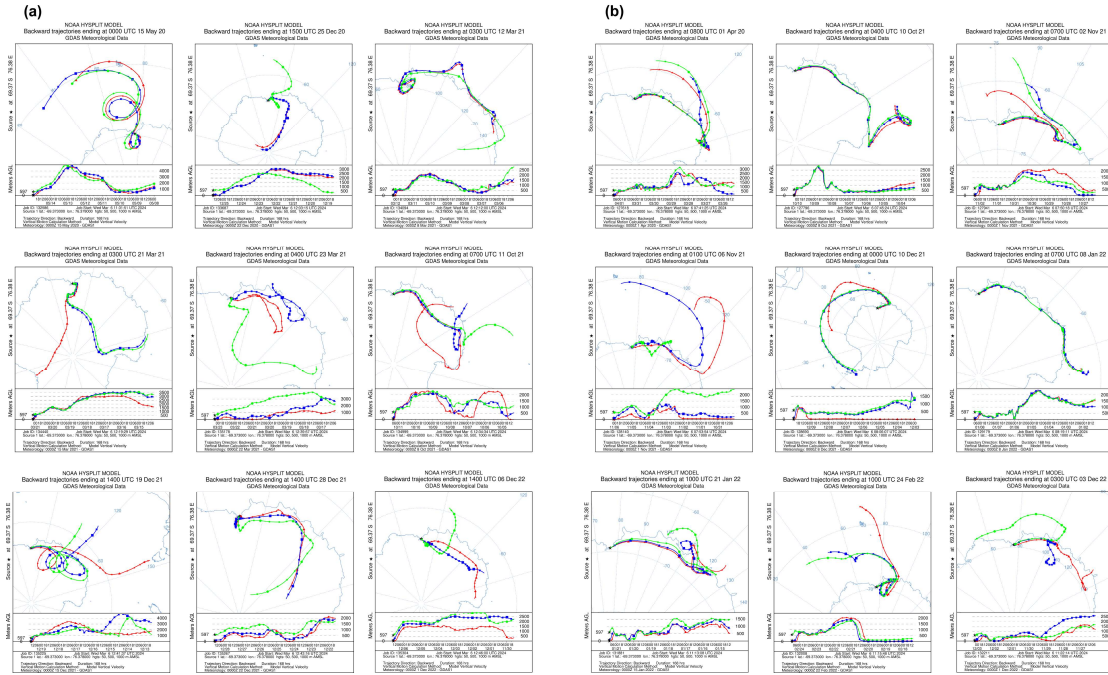


Figure S4. HYSPLIT backward trajectory of (a) low AOD days and (b) high AOD days.

Table S1. Dates are classified as low AOD days and high AOD days, respectively. Note: The fifth percentile value of the AOD daily mean is 0.02446, and days with an AOD daily mean below this value are classified as low AOD days; The 95th percentile value of the AOD daily mean is 0.14739, and days with an AOD daily mean above this value are classified as high AOD days.

| Low AOD Date | AOD _{500 nm} mean | High AOD Date | AOD _{500 nm} mean |
|--------------|----------------------------|---------------|----------------------------|
| 2020-05-15 | 0.02435 | 2020-04-01 | 0.76389 |
| 2020-12-25 | 0.02005 | 2021-10-10 | 0.32171 |
| 2021-03-12 | 0.02193 | 2021-11-02 | 0.20771 |
| 2021-03-21 | 0.0222 | 2021-11-06 | 0.16909 |
| 2021-03-23 | 0.02247 | 2021-12-10 | 0.14739 |
| 2021-10-11 | 0.02431 | 2022-01-08 | 0.17626 |
| 2021-12-19 | 0.02329 | 2022-01-21 | 0.80477 |
| 2021-12-28 | 0.02155 | 2022-02-24 | 0.34481 |
| 2022-12-6 | 0.02446 | 2022-12-3 | 0.18311 |

***The P5 of total AOD_{500 nm} mean: 0.02446** ***The P95 of total AOD_{500 nm} mean: 0.14739**